

The University of Maine

DigitalCommons@UMaine

---

Electronic Theses and Dissertations

Fogler Library

---

Spring 5-5-2023

## Disinfection Applications of On-Site Hypochlorous Acid Production

Deborah Ngabanyi Sebagisha  
deborah.sebagisha@maine.edu

Follow this and additional works at: <https://digitalcommons.library.umaine.edu/etd>



Part of the [Chemical Engineering Commons](#)

---

### Recommended Citation

Ngabanyi Sebagisha, Deborah, "Disinfection Applications of On-Site Hypochlorous Acid Production" (2023). *Electronic Theses and Dissertations*. 3775.  
<https://digitalcommons.library.umaine.edu/etd/3775>

This Open-Access Thesis is brought to you for free and open access by DigitalCommons@UMaine. It has been accepted for inclusion in Electronic Theses and Dissertations by an authorized administrator of DigitalCommons@UMaine. For more information, please contact [um.library.technical.services@maine.edu](mailto:um.library.technical.services@maine.edu).

**DISINFECTION APPLICATIONS OF ON-SITE HYPOCHLOROUS ACID  
PRODUCTION**

By

Deborah Ngabanyi Sebagisha

B.S. University of Maine, 2021

A THESIS

Submitted in Partial Fulfillment of the

Requirement for the Degree of

Master of Science

(in Chemical Engineering)

The Graduate School

The University of Maine

May 2023

Advisor Committee:

William J. DeSisto, Professor of Chemical Engineering, Advisor

Douglas W. Bousfield, Professor of Chemical Engineering

Thomas Schwartz, Associate Professor of Chemical Engineering

# **DISINFECTION APPLICATIONS OF ON-SITE HYPOCHLOROUS ACID PRODUCTION**

By Deborah Ngabanyi Sebagisha

Thesis Advisor: Dr. William J. DeSisto

An Abstract of the Thesis Presented  
In Partial Fulfillment of the Requirements for the  
Degree of Master of Science  
(in Chemical Engineering)  
May 2023

Hypochlorous acid (HOCl) is a weak acid, but strong oxidizing agent produced naturally in the human body to fight viruses and bacteria. Hypochlorous acid can be produced by electrolysis of sodium chloride and water enabling local production of disinfectant, where it is needed. Hypochlorous acid has many applications including in wound care, skin care, and disinfection of health and dental clinics. In this work, two hypochlorous acid applications were explored that could utilize local production by electrolysis. These applications were wastewater treatment and sanitization of dental operating rooms.

An electrochemical reactor and process were designed, constructed, and tested for hypochlorous acid production using wastewater effluent and sodium chloride as feed. Laboratory tests revealed important performance parameters including energy use rates and sodium chloride use rates per unit of free chlorine produced. A reactor model was developed to calculate the fractional yield of chlorine produced as a function of applied voltage to the reactor. In collaboration with Maine Manufacturing Partners, a trial of the equipment at the Biddeford Pool wastewater treatment plant was initiated.

Dental offices generate significant amounts of airborne particles during routine cleanings and surgeries (particularly periodontal work on gums and bone beneath the gums). Some office disinfection practices include fogging rooms with hypochlorous acid after procedures to neutralize airborne viruses and bacteria. Results will be shown for a finite element model of fog dispersion in a room containing airborne contaminants.

## **ACKNOWLEDGMENTS**

I would like to thank my advisor Dr. DeSisto for his kindness, encouragement, guidance, and support throughout my master's program and especially during my thesis preparation. I would like to thank Dr. Bousfield and Dr. Schwartz, my committee members, for their guidance. I appreciate my lab mate Khoa Kieu and the undergraduate students Molly Booth, Kirstie Rogers, Annemarie Toole, and Sadie Denico that I enjoyed working with.

I would like to thank Craig Cunningham and the Biddeford Pool and Saco Waste Treatment facilities for their support on my project.

To my wonderful parents and siblings, my two grandmothers, and Uncle Pascal thank you for your love, encouragement, support, and prayers from miles away. To the entire Newman Center community, thank you for being my second family.

Finally, to my friends Mary Beth, the Aylmer family, and Charles, I will forever be grateful to you.

## TABLE OF CONTENTS

ACKNOWLEDGEMENTS .....	i
LIST OF TABLES .....	iv
LIST OF FIGURES .....	vi
Chapter	
1. INTRODUCTION .....	1
1.1. Hypochlorous Acid .....	1
1.2. Electrolysis.....	1
1.3. Applications of HOCl .....	3
2. MATERIALS AND METHODS .....	5
2.1. Electrolysis Systems .....	5
2.2. Reactor Design.....	6
2.3. Batch and Continuous Experiments.....	7
2.4. Chlorine Measurement.....	7
3. BIDDERFORD POOL WASTEWATER TREATMENT PLANT TRIAL .....	10
3.1. Conventional Wastewater Treatment .....	10
3.2. UMaine and Maine Manufacturing Partners Collaboration.....	11
3.3. Opportunity and Plant Layout.....	11
3.4. Batch Testing Results.....	13
3.5. Laboratory Reactor and Process Testing.....	16
3.6. Biddeford Pool Process Trial Preliminary Design .....	21
3.7. Reactor Model.....	21
3.8. Initial Trial Results.....	28

3.9. Future Work .....	31
4. HOCl FOGGING DISPERSION .....	32
4.1. Introduction.....	32
4.2. Finite Element Model.....	33
4.3. Model Results .....	36
4.4. Applications to Dental Clinic Applications.....	40
5. CONCLUSION AND FUTURE RESEARCH DIRECTIONS .....	41
REFERENCES .....	44
BIOGRAPHY OF THE AUTHOR .....	46

## **LIST OF TABLES**

Table 1.1.	Disinfection Results from Initial Batch Trials.....	14
Table 4.2.	Fog properties .....	35



## LIST OF FIGURES

Figure 1. MMP Unit (Hypochlorous acid generator).....	5
Figure 2. Process Flow Diagram of Second Electrolysis System.....	6
Figure 3. Expanded View of Electrolysis Reactor      Figure 4. Electrolysis Reactor .....	7
Figure 5. Hach Digital Titrator (Digital Titrator Manual, Model 16900, 2013) .....	8
Figure 6. Hach Digital Titrator showing color before titration. ....	9
Figure 7. Biddeford Pool Wastewater treatment plant process flow diagram .....	12
Figure 8. Chlorine concentration change during storage for a nominal 1500 ppm batch.....	15
Figure 9. Chlorine concentration change during storage for a nominal 2000 ppm batch.....	15
Figure 10. Electrical use rate dependence on NaCl concentration. ....	16
Figure 11. Electrical use rate dependence on NaCl use rate. ....	17
Figure 12. The effect of NaCl concentration on applied voltage required to maintain 5 A current flow. ....	17
Figure 13. The effect of applied voltage on the chlorine production rate with 5 A current flow. ....	18
Figure 14. The effect of applied voltage on the chlorine current efficiency with 5 A current flow. ....	18
Figure 15. Chlorine concentration reaching steady-state during continuous operation.....	19
Figure 16. Electrical usage rate change with respect to current density for a 15 pins reactor at different NaCl concentrations. ....	20
Figure 17. CSTR model of the MMP chlorine generation unit. ....	22
Figure 18. Schematic of the Electrolysis Reactor showing chemical reactions at the cathode and anode.....	22
Figure 19. I-V curves for a typical reactor with different NaCl concentrations. ....	24

Figure 20. Voltage vs chlorine fractional yield .....	27
Figure 21. Reduction in energy use using increased reactor area at lower voltage. ....	28
Figure 22. MMP Dirigo Stream Unit and buffer tank at Biddeford Pool Plant. ....	29
Figure 23. Plant flow and respective chlorine metering flow during morning hours at Biddeford Pool. ....	30
Figure 24. Corresponding salt use and residual chlorine for morning hours at Biddeford Pool. ....	30
Figure 25. Sensitivity of chlorine reading to pH for Walchem high Cl <sub>2</sub> sensor.....	31
Figure 26. Geometry of a room and fogger location .....	35
Figure 27. Boundaries of the room .....	36
Figure 28. Extra Coarse mesh.....	37
Figure 29. 1 fog inlet at 0.05 m/s inlet velocity .....	38
Figure 30. 1 fog inlet at 0.5 m/s inlet velocity .....	38
Figure 31. 1 fog inlet at 0.05 m/s velocity after 1000s~17min. ....	39
Figure 32. 2 fog inlets at 0.5 m/s inlet velocity .....	40
Figure 33. 2 fog inlets at 0.05 m/s inlet velocity .....	40

## CHAPTER 1

### INTRODUCTION

#### 1.1 Hypochlorous Acid

Hypochlorous acid (HOCl) is a weak acid that forms when chlorine dissolves in water. It is primarily a disinfectant, it has antimicrobial, antiseptic, and antifungal properties. HOCl is produced in mammal's white blood cells to fight against pathogens. HOCl is a powerful oxidizing agent. In acidic to neutral aqueous state (pH 5-7), HOCl, the strongest chlorine species, reaches over around 80% of Active free chlorine (AFC) and its sterilizing power is over 80 times more than sodium hypochlorite (NaOCl) or bleach (Bajgai, et al., 2020). Researchers Wang et al describe the production, stabilization, and biological activity of HOCl. The pH must be maintained at 3.5 to 5 to maintain HOCl in a stable form, to maximize its microbial activities, and minimize undesirable side products. At pH less than 3.5, the mixture of chlorine gas, trichloride, HOCl exists. At higher pH hypochlorite ion ( $\text{OCl}^-$ ) is formed and becomes predominant.

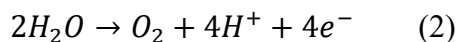
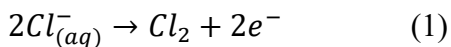
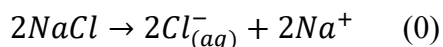
When our body encounters bacteria, it naturally releases hypochlorous acid to fight infection. HOCl's neutral charge allows it to easily penetrate the pathogen cell, to reach the DNA of the cell and to destroy it. Hypochlorite ( $\text{OCl}^-$ ) on the other hand is negatively charged, it repels with the microbe cell and does not penetrate the microbe cell. Hypochlorous acid can be produced commercially by electrolysis of sodium chloride and water.

#### 1.2 Electrolysis

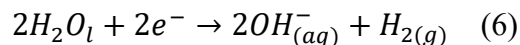
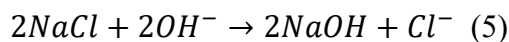
Electrolysis is the decomposition of a substance by an electric current process, for example, splitting water into hydrogen and oxygen by electricity. The electrolysis of salt (NaCl)

occurs by dissociating sodium ions ( $\text{Na}^+$ ) and chloride ( $\text{Cl}^-$ ) ions with the formation of hydroxide ( $\text{OH}^-$ ) and hydrogen ( $\text{H}^+$ ) ions in the solution. (Ampiaaw, Yaqub, & Lee, 2021). When an electric current passes through the solution, electrons move from the anode to the cathode. The negatively charged ions move towards the anode where oxidation occurs to produce  $\text{HOCl}$ ,  $\text{ClO}^-$ ,  $\text{HCl}$ , oxygen ( $\text{O}_2$ ) and Chlorine ( $\text{Cl}_2$ ) gas (see equation 1, 2, and 3). Once chlorine gas is formed in equation 1 it directly reacts with water to form  $\text{HOCl}$  (equation 3). The positive ions move to the cathode to form sodium hydroxide and hydrogen (equations 5 and 6).

Reactions at the anode:



Reactions at the cathode:



$\text{HOCl}$  can be produced by one of three methods: electrolysis of salt water, hydrolysis of chlorine gas, and acidification of hypochlorite.

Equation 3 above shows the formation of  $\text{HOCl}$  by hydrolysis of chlorine gas. This reaction is limited by the hazards of handling chlorine and difficulty in manipulation it.

The disadvantage of electrolysis method in equation 2 is the difficulty in controlling the target concentration. Challenges with diluting concentrated hypochlorite with acid include handling hazardous chemicals, although some consider it a preferred method of producing hypochlorous acid (Wang, et al., 2017). This thesis is focused on electrolysis production to reduce handling of hazardous chemicals and reduce supply chain dependencies.

A typical electrolysis reaction involves the transfer of charge between an electrode and a chemical species. The reaction has a cell potential energy which is the minimum energy for the reaction to occur. The cell potential for half-reaction (1) is  $E_0 = 1.3583 \text{ V}$ . The cell potential for half-reaction (6) is  $E_0 = -0.8277 \text{ V}$  resulting in an overall cell potential of  $2.186 \text{ V}$ . (Perry et al., 2020)

Additionally, two types of overpotentials exist which increases the minimum voltage required for reaction. A kinetic charge transfer limitation overpotential which can be minimized by catalyst selection, and concentration overpotentials, caused by mass-transfer limitations of species to and from the electrode surface. These limitations are more prominent at higher current densities. Reactions involving bubble formation on the electrode surface (and its slow removal) can also affect the number of available reaction sites and mass-transfer limitations. Finally, the overall ohmic resistance of the reactor, a function of electrical connections, electrode gap, electrode geometry, etc. Impacts the minimum voltage required for reaction.

### **1.3 Applications of HOCl**

HOCl is being used in eye care, wound care, and skin care products, in hospital and dental clinics as cleaning solutions, in wastewater treatment facilities, in swimming pools, and in fogging for disinfection. In eye care, HOCl helps to relieve dry and itchy eyes. Hypochlorous

acid is used for the treatment of blepharitis and chronic dry eyes (Bahoshy, 2018). Blepharitis is the inflammation of the eyelid; it is caused by the growth of bacteria around the eyelids.

Stabilized HOCl was found to be nonirritating in rabbit eye and non-sensitizing in guinea pig animal models (Wang, et al., 2017). HOCl can be used as a hand sanitizer. Research indicates HOCl based hand sanitizers have the potential to be better than alcohol-based hands sanitizers in sanitizing human skin and hands (HOCl Inside, 2023). In agriculture, hypochlorous acid is used in irrigation systems for microbial control on plant and fruit crops (CleanLink). HOCl is safe for use on all animals. It is the most effective remedy for open and minor wounds, for dry skin and rashes, and for managing animals ear infection (Clieron, 2021).

## CHAPTER 2

### MATERIALS AND METHODS

#### 2.1 Electrolysis Systems

A system for producing hypochlorous acid by sodium chloride/water electrolysis was purchased from Maine Manufacturing Partners (MMP). The unit recirculates the NaCl/water solution through a reactor, where electricity is applied to produce hypochlorous acid and hydrogen. The hydrogen is collected by filtration through a ceramic hollow fiber membrane and quantified by water displacement. The circulating solution also passed through a bag filter.



Figure 1. MMP Unit (Hypochlorous acid generator)

A simpler system shown in Figure 2 was assembled that included a 10-gallon holding tank, a recirculating pump, a reactor and power supply. Both systems were used for batch reactions. The first system was used for continuous reactions.

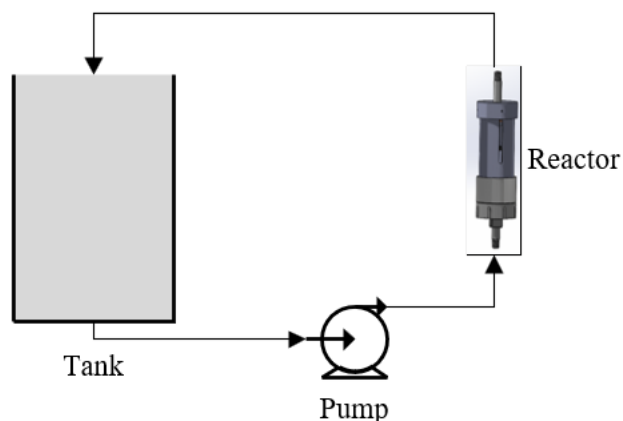


Figure 2. Process Flow Diagram of Second Electrolysis System

## 2.2 Reactor Design

An electrochemical reactor was designed and fabricated for testing. The design was focused on plumbing compatibility, to keep costs down and ease scale-up. The outside part of the electrolysis reactor in figure 4 is made of PVC. The inside part has the anode and the cathode which can be made of different materials. Reactors made of different cathode and anode materials were tested in the lab. The reactor made with titanium (Ti) coated with Mixed Metal Oxide (MMO) and Ti has proved to be the best. Other reactor designs were made of MMO and Carbon, MMO and Iron-Titanium.



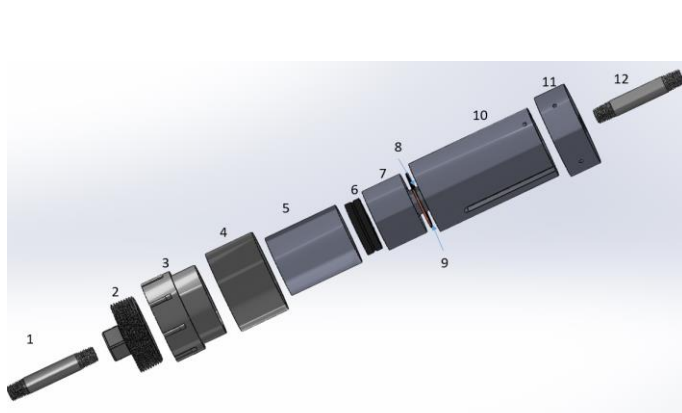


Figure 3. Expanded View of Electrolysis Reactor



Figure 4. Electrolysis Reactor

### 2.3 Batch and Continuous Experiments

In a typical batch experiment, NaCl (McMaster, Carr, 99.8%) was weighed to appropriate amounts, followed by addition of deionized water to prepare solutions ranging from 2.5 to 40 g/L in concentration. This solution was fed to the system which held approximately 6 Liters.

Typically, a constant current was applied with a DC power supply (BK Precision, 30 A) from 3 to 10 A. The reaction was allowed to proceed, typically one hour, followed by power removal.

For continuous experiments, a constant supply of NaCl/water was supplied with a peristaltic pump with flow rates between 60 and 200 mL/min. A product stream was withdrawn from the system at the same rate. The recirculation pump recycled most of the solution back through the reactor. Exit flow rates were periodically measured with a bucket and stopwatch method. Chlorine concentration was measured periodically (every 15 minutes or so) during the run. Runs typically took several hours to complete.

### 2.4 Chlorine Measurement

Chlorine concentration was measured during and after process runs, both in batch and continuous. The measurement technique used measured total free chlorine concentration which

included both  $\text{HOCl}$  and  $\text{OCl}^-$  from equation (4) as mg of  $\text{Cl}_2$  per L of solution or parts per million, ppm. The total free chlorine was measured by iodometric titration. Potassium Iodide reacts with free chlorine to release free iodine at pH lower than 8. The free iodine is titrated with sodium thiosulfate (Digital Titrator Manual, Model 16900, 2013). The Digital Titrator is shown in Figure 5. The free iodine solution is shown in Figure 4 prior to titration.

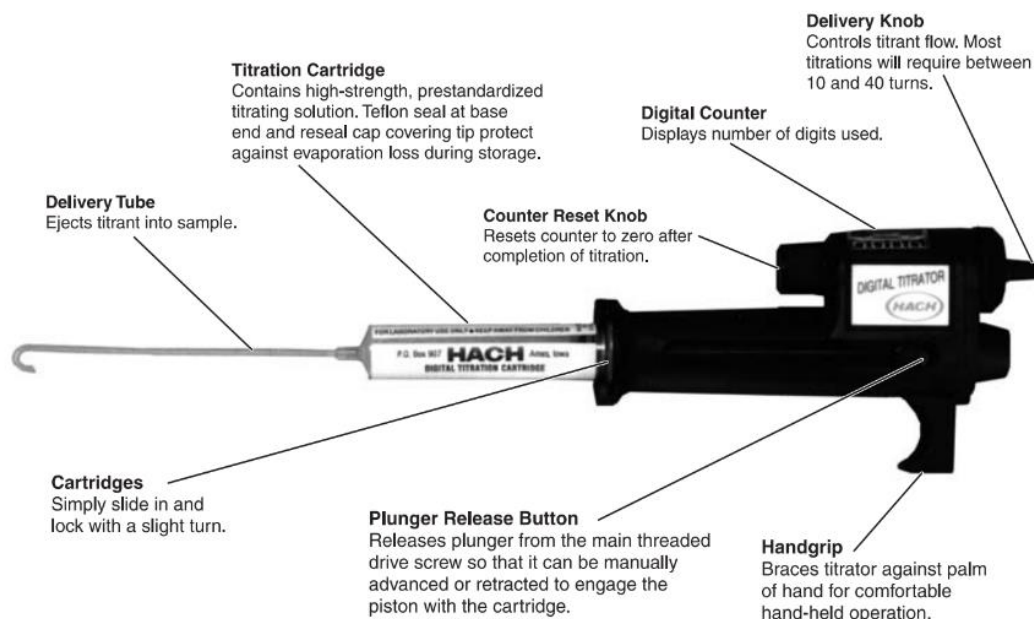


Figure 5. Hach Digital Titrator (*Digital Titrator Manual, Model 16900, 2013*)



Figure 6. Hach Digital Titrator showing color before titration.

The following procedure was used to determine chlorine concentration:

1. Weight on 1 g of HOCl and add deionized water up to 50 g.
2. Mix the two then add 1 oxygen powder pillow (Hach), 1 Potassium Iodide pillow (Hach), and 3-5 drops of starch indicator solution (Hach).
3. Add drops of Sodium Thiosulfate Standard Solution (0.113 N sodium thiosulfate, Hach) until the solution turns clear.
4. Read the number on the pipettor and multiply it by 5 to find the final  $\text{Cl}_2$  concentration in ppm.

## **CHAPTER 3**

### **BIDDEFORD POOL WASTEWATER TREATMENT PLANT TRIAL**

#### **3.1 Conventional Wastewater Treatment**

Wastewater treatment plants treat water from sewers, homes, and businesses. This treatment process consists of physical, chemical, and biological processes to remove solids and organic matter to meet water quality standards. The first step is preliminary treatment, it consists of removing coarse solids and other large materials in wastewater through screening or comminution in some cases. The primary treatment removes settleable organic and inorganic solids by sedimentation or skimming. Approximately 25 to 50% of the incoming biochemical oxygen demand (BOD), 50 to 70% of total suspended solids and 65 % of the oil and grease are removed during this step (Pescod, 1992). Biochemical Oxygen Demand is the amount of dissolved oxygen that must be present in water for microorganisms to decompose the organic matter in the water (School, 2018). BOD removal in wastewater is important because it affects the quality of water. Less BOD in water implies less oxygen or food for organic matter or microorganisms. The secondary treatment or second sedimentation removes biodegradable dissolved and colloidal organic matter using aerobic biological treatment processes. The aerobic biological treatment consists of metabolizing organic matter by injecting air that contains oxygen and microorganisms. After this step, 85% of BOD, suspended solids, and some heavy metals are removed. The solids removed from the primary and secondary sedimentation form the sludge processed and removed from it. The Disinfection step consists of applying a disinfectant in the disinfection tank. The chlorination tank provides a contact time of about 30 minutes. The killing effects of the disinfectant depend on pH, contact time in the disinfection tank, the amount of organic content, and effluent temperature.

### **3.2 UMaine and Maine Manufacturing Partners Collaboration**

The UMaine Applied Electrolysis Laboratory (AEL) is in collaboration with Maine Manufacturing Partners (MMP) to develop and deploy technology focused on utilizing wastewater to generate useful chemicals. An example includes utilizing wastewater to generate chlorine (in the form of hypochlorous acid) and hydrogen by electrolysis. Our vision is to flip the value of wastewater.

To this end, systems and components have been designed, constructed, and tested to directly intake wastewater effluent and sodium chloride to efficiently and economically produce hypochlorous acid and hydrogen. The hypochlorous acid will be used as a disinfectant. The system is plumbing compatible, robust, and scalable.

A system manufactured by MMP (Dirigo Stream™) is under testing and evaluation at the Biddeford Pool treatment plant. In support of this trial, UMaine AEL has collaborated on system design, integration, data collection, and data evaluation. This chapter reports on laboratory efforts to support this trial while seeking continual improvement in technology and operation.

A preview of the chapter includes: a review of the opportunity; a description of the current plant process and layout; challenges with using concentration bleach; initial batch trial results; hypochlorous acid stability; laboratory data to support the trial; a rate model; and initial trial results and analysis.

### **3.3 Opportunity and Plant Layout**

Biddeford Pool is a small wastewater treatment plant in Biddeford Maine sized to treat up to approximately 20,000 gallons of wastewater daily. The plant layout is shown in Figure 7.

Wastewater is collected in a box tank, then moved to the Rotating Biological Contactors (RBCs)

for biological treatment. The RBCs are comprised of rotating disks mounted on a horizontal shaft. The media slowly rotates while creating bacterial growth on the disks. The disks are partially submerged in the flowing wastewater in the reactor. The rotation between air and wastewater allows for appropriate aeration and degradation of the bacteria.

Effluent from the RBCs flow into two clarifiers in series. The sludge from the two clarifiers is pumped and stored into a sludge tank. The effluent from the second clarifier is contacted with disinfectant (dilute bleach) metered from the bleach tank into the disinfection tank. After disinfection the effluent is sent into the environment. The effluent is required to have minimal to zero bacteria and free chlorine levels below 1 ppm. In order to manage this, the free chlorine concentration at the disinfection tank entry is maintained at 1 ppm by feedback control to a feed pump connected to the bleach tank. Biddeford Pool's plant uses dilute bleach at approximately 0.6 % strength.

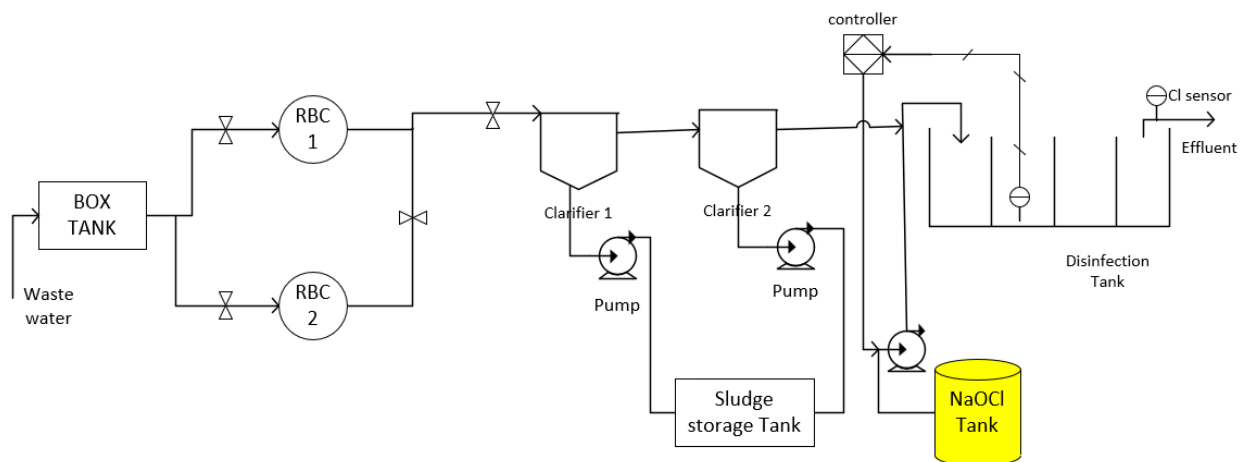


Figure 7. Biddeford Pool Wastewater treatment plant process flow diagram

The Biddeford Pool Wastewater Treatment Plant provided an opportunity to integrate an on-demand chlorine generation system to meet plant disinfection needs. There are several advantages to on-site disinfection generation. The first is plant safety. The delivery, storage, and handling of concentrated bleach (12.5%) is eliminated. Concentrated bleach is corrosive and hazardous to handle. Hypochlorous acid generated on site uses sodium chloride, water, and electricity to generate lower concentrations of disinfectant to eliminate large storage vessels and weekly delivery. Secondly, on-site generation removes the dependency on a supply chain where concentrated bleach is manufactured off-site, then delivered in bulk. This removes uncertainty in supply chain disruptions as well as fluctuating prices.

### **3.4 Batch Testing Results**

Prior to integrating an on-site generation unit, batch testing was performed using hypochlorous acid produced in our laboratory. We produced 5-gallon batches with free chlorine concentrations ranging from 1500 to 2500 ppm and pH from 6 to 8. The metering pump (Figure 5) inlet was connected to the 5-gallon batch material during plant operation. Bacterial kill was measured. Data from these experiments is shown in Table 1. MMP/AEL HOCl is the batch material produced in our lab and compared to the existing bleach process. Pump flow is the disinfectant metering rate into the disinfection tank. Metering flows for the batch material were greater relative to plant flow when compared with the bleach. The main reason for this is twofold: the bleach concentration (free chlorine) is about 5-6 times higher than the free chlorine concentration in our laboratory produced material; and the control process was not tuned to the lower concentrations of batch material. The higher residual chlorine level in row 4 of the data reflects the poor process control. This number is normally kept at or below 1.0 ppm  $\text{Cl}_2$ . The batch material destruction of Fecal Coliform and of Enterococci were excellent. Enterococci is

an unsafe bacteria that impacts recreational waters and is being looked at for removal by the Maine Department of Environmental Protection. **(Private communication with Plant Directors from Saco and Biddeford Pool)**

Table 1.1. Disinfection Results from Initial Batch Trials

Disinfection Results from Initial Batch Trials							
Disinfectant	Plant Flow (GPM)	Pump Flow (GPH)	Influent Total Residual Chlorine (ppm)	Effluent Total Residual Chlorine (ppm)	Total Suspended Solids	Fecal Coliform	Enterococci
NaOCl (Bleach)	3.8	0.124	0.98	0.93	4.9	1	37
MMP/AEL HOCl	4.44	0.887	0.91	0.88	4.6	<1.0	8.6
NaOCl (Bleach)	3.36	0.193	1.02	0.96	2.2	<1.0	12.1
MMP/AEL HOCl	2.59	0.763	1.47	0.94	3.2	<1.0	7.1

Hypochlorous acid is an unstable molecule in the presence of heat and UV light (Ishihara et al., 2017). The stability of higher concentration solutions was monitored to assess short-term storage options. Of four batch solutions tested at the plant, smaller volumes (250 mL) were stored in opaque containers in the lab. Chlorine concentrations were measured daily. Results are shown in Figures 8 and 9. The lower pH samples were more sensitive to degradation than the higher pH samples. In the case of lower pH, the ~1500 ppm sample degraded 5% after one day and 8.5% after 4 days. The ~2000 ppm sample degraded 5% after one day and 14% after 4 days. This is important to consider for short term storage in a buffer tank at the plant.



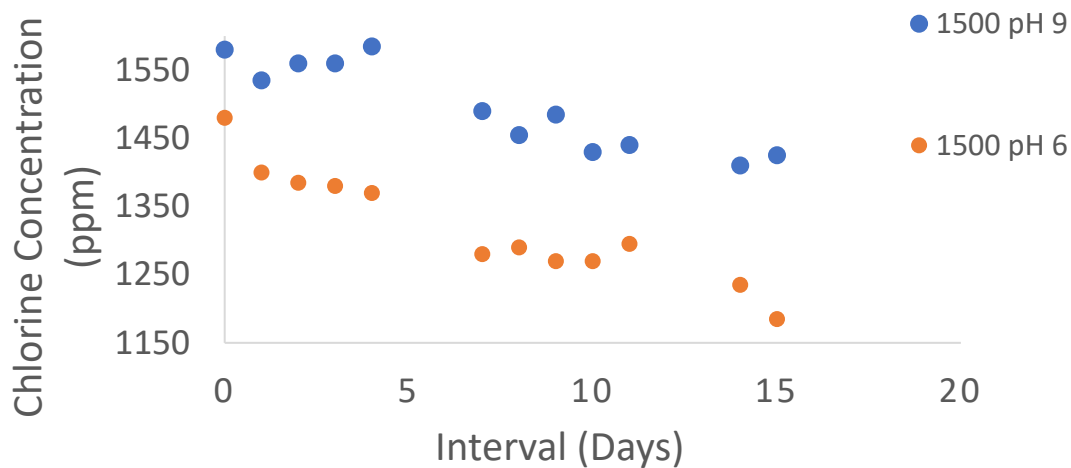


Figure 8. Chlorine concentration change during storage for a nominal 1500 ppm batch.

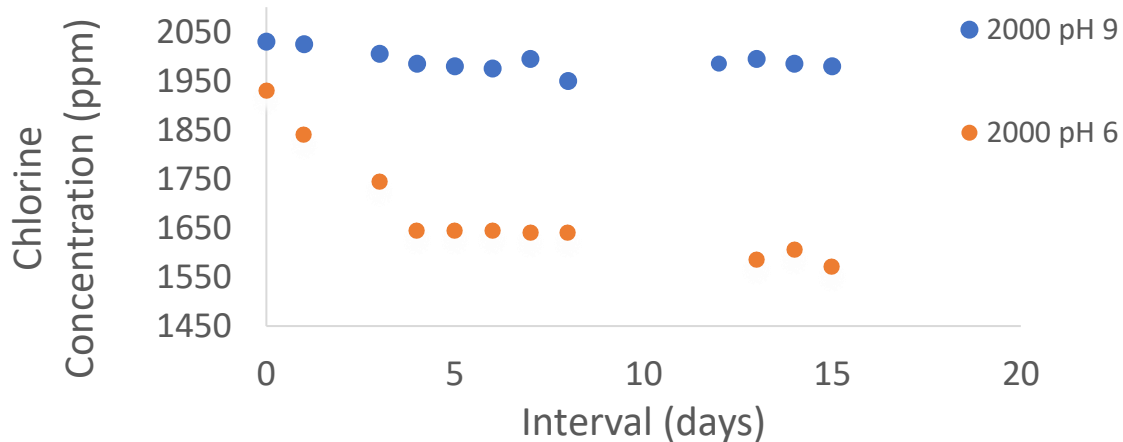


Figure 9. Chlorine concentration change during storage for a nominal 2000 ppm batch.

Prior to on-site generation design, the chlorine demand must be estimated at the plant. Based on meetings with plant operators, a bleach dilution procedure was estimated along with typical bleach tank refill schedules. From this information a chlorine demand of 0.13 g/min was estimated. Because flow rates can vary quite a bit, the initial design was for 0.2 g/min of

chlorine. In reality, the plant flows can vary considerably, although are tempered somewhat in this particular plant because of flow balancing capabilities.

### 3.5 Laboratory Reactor and Process Testing

Laboratory experiments were conducted to evaluate electrochemical reactor performance as a function of several different variables. The initial goal was to determine the reactor size required to meet demand. The variables included salt concentration, flow rate, applied voltage, current density, and electrode geometry.

Testing included running the system in batch or continuous mode. Some basic reactor/system relationships are shown below. These particular experiments were conducted at 5 Amps current (constant current mode) or  $1000 \text{ mA/cm}^2$  and run for 60 minutes. The chlorine concentration was measured after the run terminated. Figure 10 shows the relationship between electrical use rate and salt concentration. As salt concentration increases, the solution resistance decreases, requiring less voltage to produce the same current through circuit. A plot of the tradeoff between electrical and salt usage is shown in Figure 11.

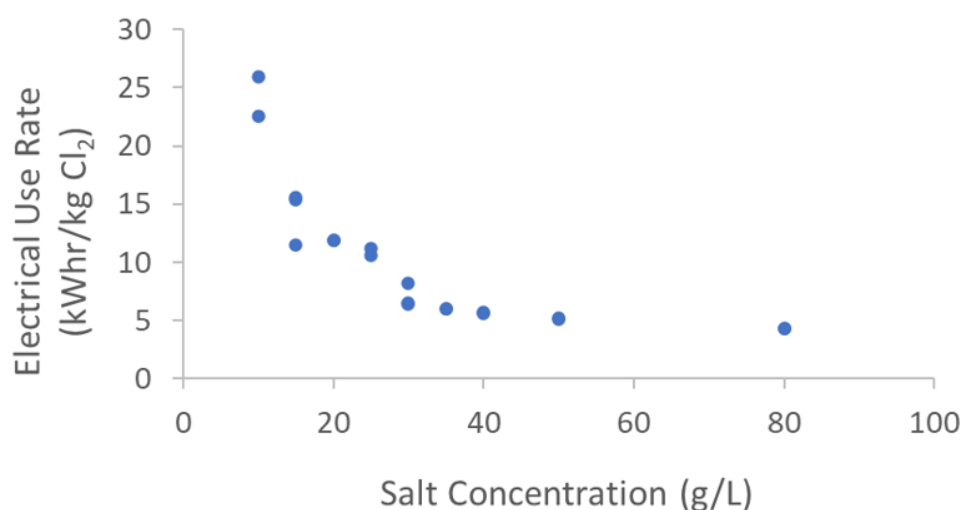


Figure 10. Electrical use rate dependence on NaCl concentration.

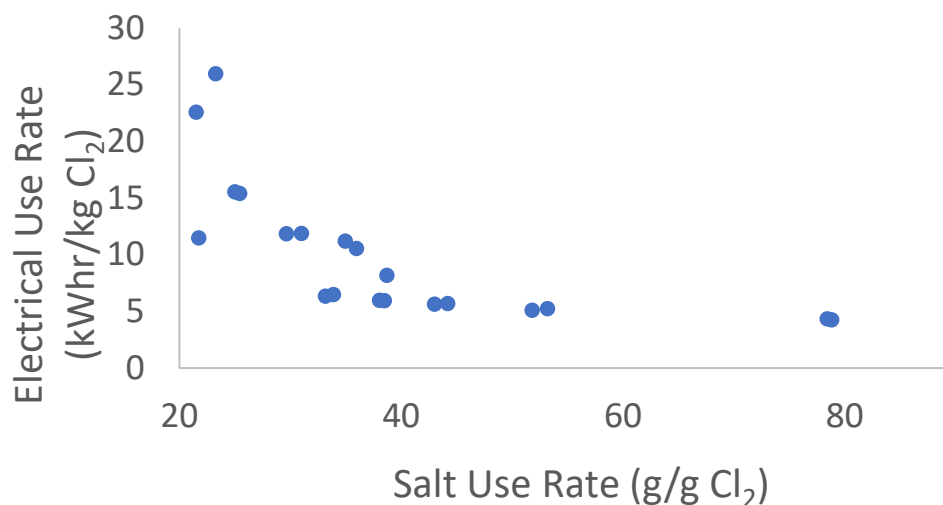


Figure 11. Electrical use rate dependence on NaCl use rate.

As salt concentration decreases a higher applied voltage is required to maintain constant current. For the same data set above, the current flow through the same reactor was 5 Amps. The effect on the voltage is shown in Figure 12.

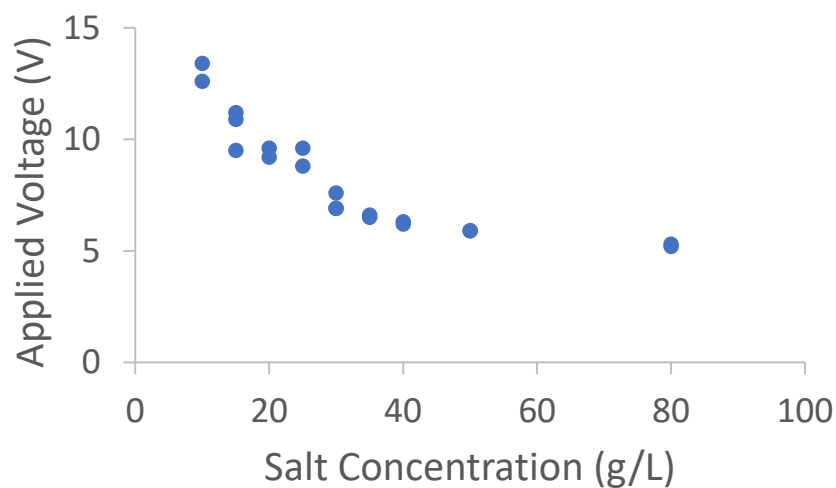


Figure 12. The effect of NaCl concentration on applied voltage required to maintain 5 A current flow.

The relationship between the applied voltage and chlorine production rate and chlorine current efficiency are shown in Figures 13 and 14. The chlorine current efficiency is defined as the

fraction of current used to produce chlorine relative to theoretical amount of chlorine produced at the same current. An explanation for this relationship involves the competing anodic reaction forming oxygen instead of chlorine at higher voltages. This is analyzed further below.

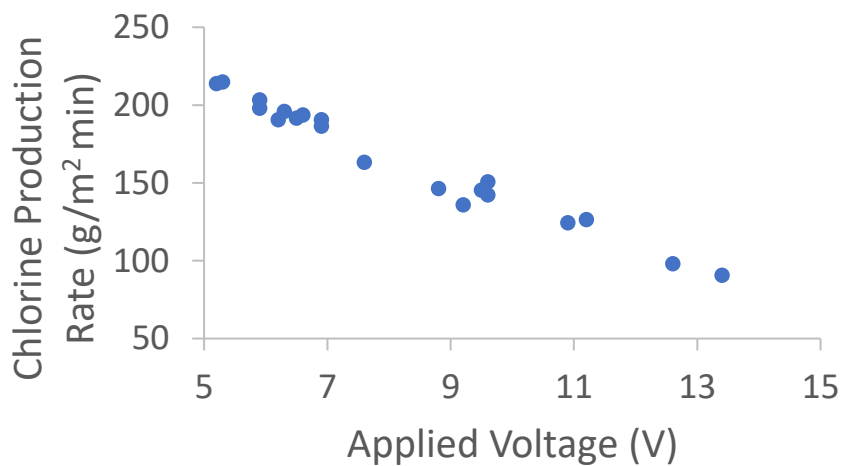


Figure 13. The effect of applied voltage on the chlorine production rate with 5 A current flow.

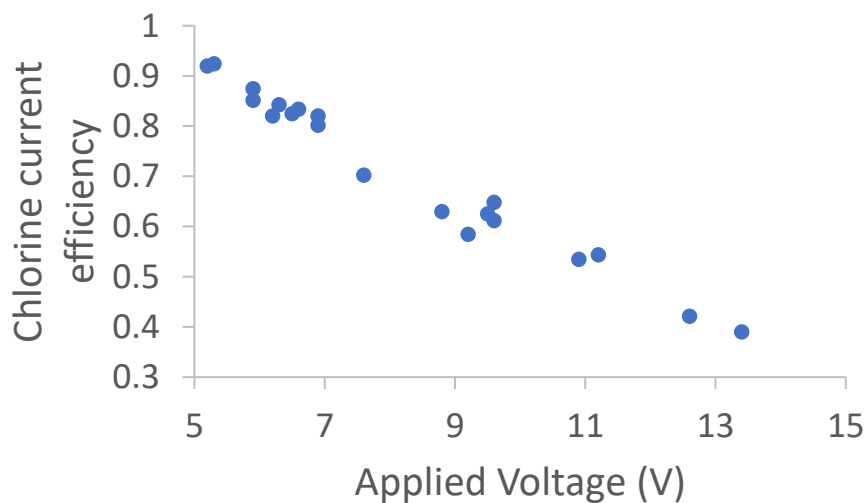


Figure 14. The effect of applied voltage on the chlorine current efficiency with 5 A current flow.

A significant number of experiments were conducted in continuous operation, where a steady flow of product was withdrawn, replaced by an equal flow of sodium chloride solution, under constant current conditions. For these experiments a wider range of current densities were examined. Data for production rate was collected at steady-state. A typical plot of chlorine concentration vs time reveals the steady-state region of the experiment as shown in Figure 15 (from Test Plan/Continuous Run). This particular experiment was run at 7 Amps, 20 g/L NaCl, and 260 mL/min flow.

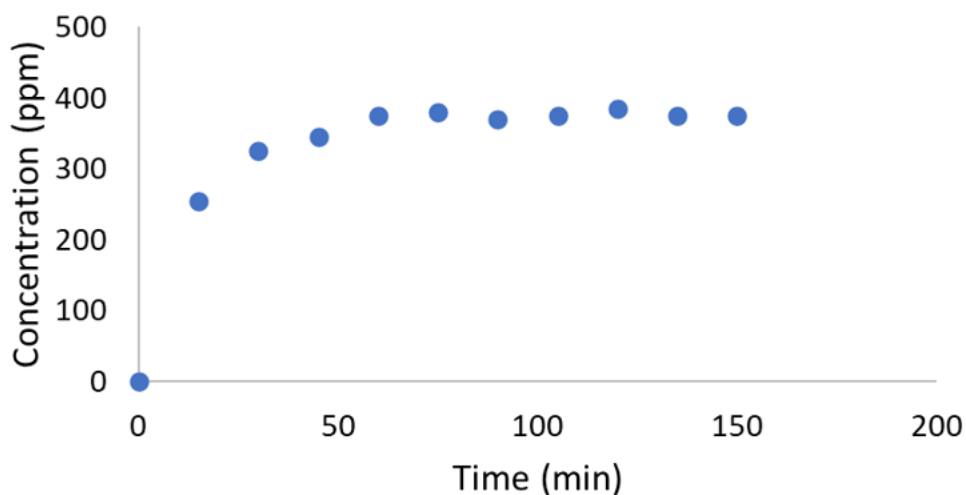


Figure 15. Chlorine concentration reaching steady-state during continuous operation

The electrical use rate related to current flow at different salt concentrations is shown in Fig. 16.

The electric use rate increases linearly with current density at 0.001425 m<sup>2</sup> electrode area. The electric use rate is more sensitive to current flow at lower salt concentrations. In the section below, a rate model is developed to help explain these relationships.

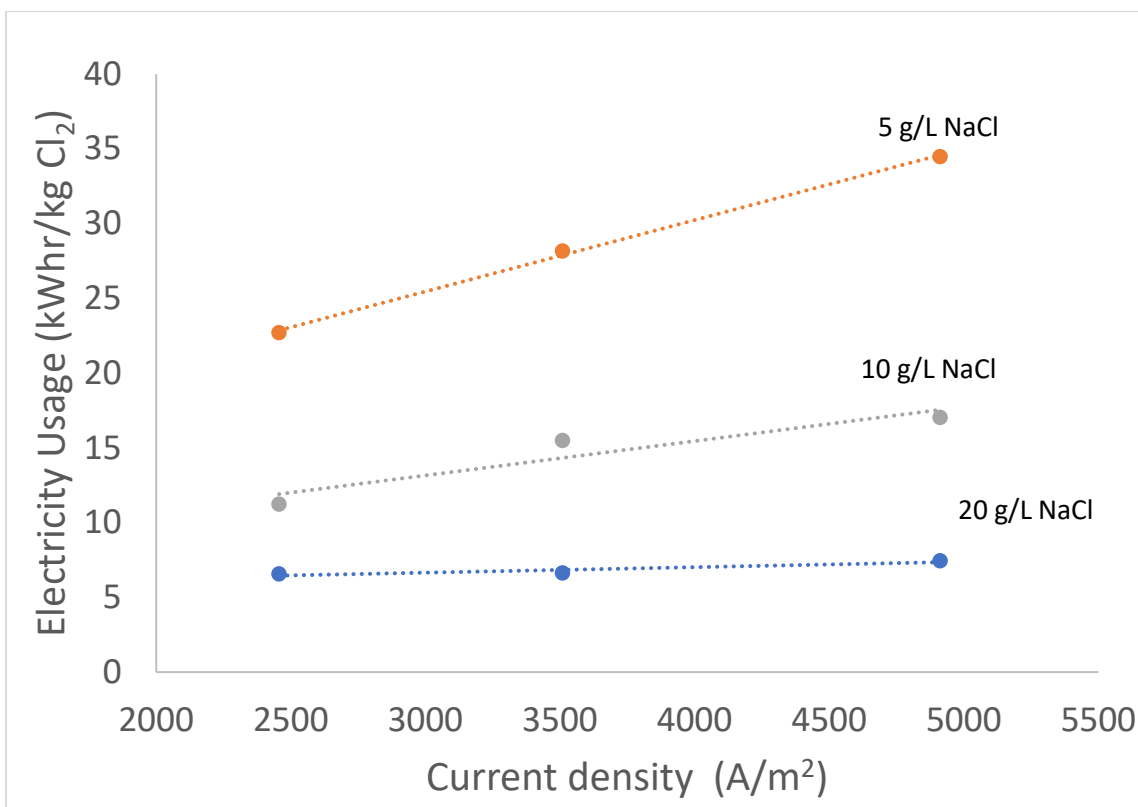


Figure 16. Electrical usage rate change with respect to current density for a 0.001425 m<sup>2</sup> reactor at different NaCl concentrations.

### 3.6 Biddeford Pool Process Trial Preliminary Design

The goal is to replace the bleach tank in Figure 7 with an on-site disinfectant generation system. Because the plant flow is uneven throughout the day and season, a buffer tank is used. Ideally, the buffer tank will be maintained with appropriate levels of chlorine (either HOCl, OCl<sup>-</sup>, or both) which is withdrawn under process control to kill bacteria in the chlorination tank prior to discharge (see Fig. 7). The tank is replenished with NaCl/water. To replenish the withdrawn chlorine, the solution in the buffer tank is circulated through an electrolysis reactor which converts chloride ions (from the incoming NaCl solution) to chlorine. The “electrochemical reactor” can be configured as several smaller reactors either in parallel or series, to address

overall plant demand. Recall an initial plant disinfectant demand was estimated at 0.2 gm  $\text{Cl}_2/\text{min}$ .

Because the system is integrated into the treatment plant, it is important to maintain reasonably steady chlorine concentration in the buffer tank. The plant's disinfectant metering process control system is tuned to a narrow range of withdrawal rates. If the buffer tank concentration changes significantly, the metering flow rate will require greater change also, leading to less-than-optimal control. This could result in overshoot, where excess chlorine will require sodium bisulfite neutralization prior to discharge. Or undershoot, resulting in incomplete bacterial kill, unsafe for the environment.

### **3.7 Reactor Model**

The buffer tank/reactor combination, shown in Figure 17 can be modeled as a continuous-stirred tank reactor or CSTR. The electrochemical reactor is shown in Figure 18. The NaCl has two roles: it provides  $\text{Cl}^-$  as a reactant and provides ionic conductivity to complete the electric circuit. NaCl concentration impacts overall circuit resistance and impacts power use. Approximately 10% of the  $\text{Cl}^-$  is converted to chlorine product.

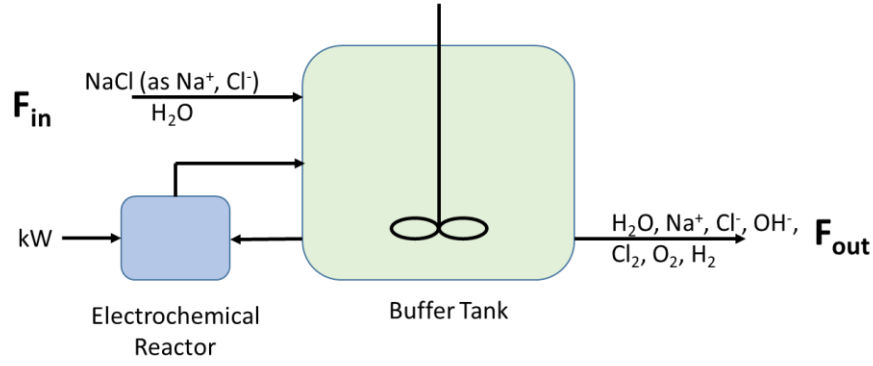


Figure 17. CSTR model of the MMP chlorine generation unit.

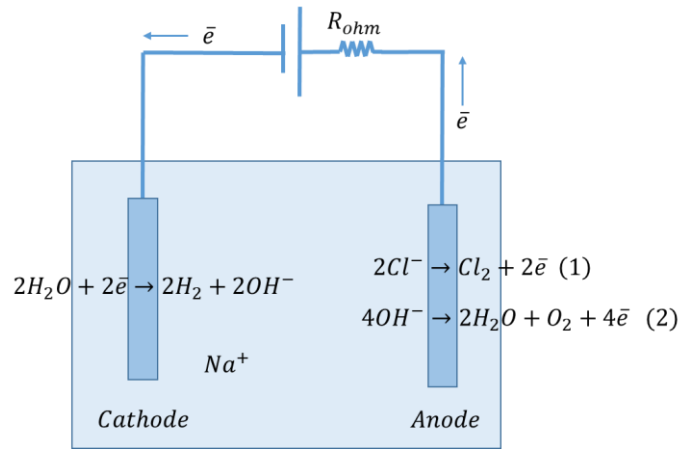


Figure 18. Schematic of the Electrolysis Reactor showing chemical reactions at the cathode and anode.

The overall and chlorine product mass balances for the CSTR in Fig. 17 are:

$$F_{in} = F_{out} \text{ units mass/time}$$

$$r_{Cl_2} \cdot M_{Cl_2} = C_{Cl_2} \cdot \dot{V}_{out} \text{ units mass/time}$$



where  $r_{Cl_2} = \frac{\phi j A}{2F}$  with units of mol/time. The fractional yield is  $\phi$ ;  $j$  is the current density;  $A$  is the electrode area,  $M$  is the molecular weight; and  $F$ , is the Faraday constant. The flow rate of NaCl into the buffer tank is equal to  $C_{NaCl} \cdot \dot{V}_{out}$ . Concentrations are in units of mass/volume and  $\dot{V}_{in}$  and  $\dot{V}_{out}$  are volumetric flow rates. Chlorine concentrations are typically given in mg/L or ppm. It is desirable to maintain a constant salt flow rate into the buffer tank to maintain a constant salt concentration within the buffer tank.

The withdrawal rate from the buffer tank is a function of the bacterial load which generally correlates with plant flow. For similar bacterial loads,  $F_{out}$  will be constant, assuming there is no other unexpected entity that scavenges free chlorine. The volumetric flow rate out of the tank is inversely related to the chlorine concentration at fixed chlorine demand. Since this flow is balanced by the flow of NaCl into the tank, NaCl consumption is reduced at higher buffer tank concentrations. The tradeoff of keeping higher concentrations is lower tank turnover and risking losing some chlorine to natural degradation (see Fig. 8).

The second process input is electricity used to generate chlorine. An initial approach to reducing electrical cost is minimizing ohmic losses in the system. Ohmic resistance comes from materials choice, electrical connections, electrode gap, and solution conductivity. For a typical reactor, the relationship between current and voltage is shown in Figure 17 for different salt concentrations. There is no current flow until near 3 V. The minimum voltage for reaction is 2.3 V from the reactions in Fig. 16

There is some overpotential required to initiate the reactions as well. In these plots, between 4 and 9 Volts the relationship between current and voltage is quite linear or ohmic. The conductivity (slope), expectedly, is dependent on salt concentration.

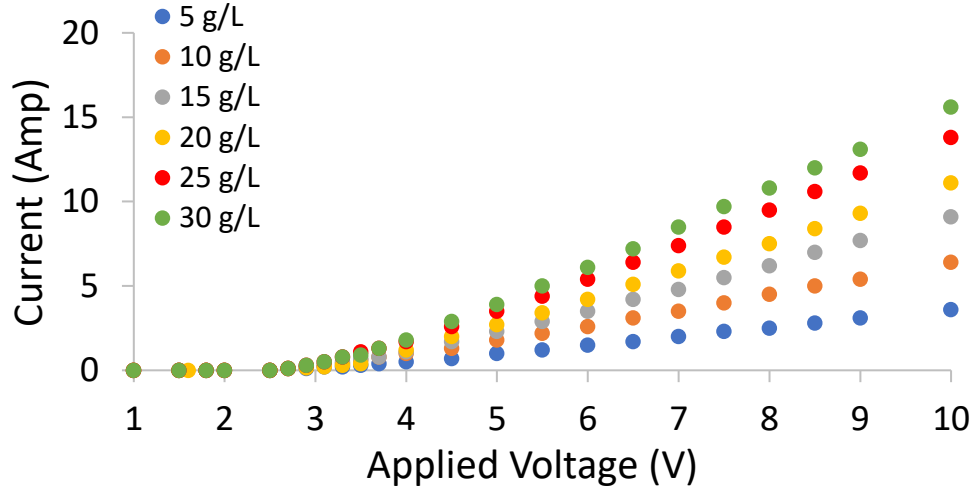
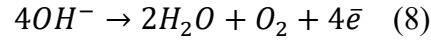
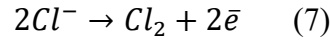


Figure 19. I-V curves for a typical reactor with different NaCl concentrations.

The two primary anodic half-reactions are shown below:



The current flowing through the circuit can either produce chlorine or oxygen. Extra voltage is required for higher ohmic resistance which arises from salt concentration, electrode gap, electrical connections, etc. To simplify the model, only the above reactions are considered and the overall resistance through each pathway is approximated by the ohmic resistance,  $R_{ohm}$ .

An energy balance is written as:

$$IV = I_1^2 R + I_2^2 R \quad (9)$$

Where  $I_1$  is the current involved in (7) and  $I_2$  is the current involved in (8).  $R$  is estimated by  $R_{ohm}$ . The fractional yield of (7) is  $\phi$  giving the expression for reaction (7):

$$r_1 = \frac{\phi j_1 A}{2F} \quad (10)$$

The selectivity is  $\theta = \frac{r_1}{r_2}$  (11) and related to fractional yield  $\theta = \frac{\phi}{1-\phi}$  (12).

Where  $j_1$  is the current density,  $A$  is the electrode surface area and  $F$  is the Faraday constant with units  $Amp \cdot s/mol$  which can be converted to  $Amp \cdot s/kg$  using molecular weight. The current contributing to reaction (7) is equal to  $j_1 A$ . Rewriting the energy balance (9) in terms of  $r_1$  and normalizing the input power to  $r_1$  yields:

$$\frac{(IV)A}{2r_1 F} = j_1 A^2 R + \frac{j_1 A^2 R}{\theta^2} \quad (13)$$

Further simplification of (7) results in:

$$\frac{P}{r_1} = 2FR\phi \left(1 + \frac{1}{\theta^2}\right) jA \quad (14)$$

Where  $P$  is the input power and  $\frac{P}{r_1}$  is the electric usage metric with units  $kW \cdot hr/kg Cl_2$ .

A plot of  $\frac{P}{r_1}$  vs.  $j$  of experimental data collected during continuous runs at steady-state under different salt concentrations is shown in Figure X above. The slope of the line is:

$$2FR\phi \left(1 + \frac{1}{\theta^2}\right) A \quad (15)$$

Equation (15) is written more conveniently as:

$$\frac{P}{r_1} = 2FR\beta jA \quad (16)$$

where:

$$\beta = \phi + \frac{(1-\phi)^2}{\phi} \quad (17)$$

As the voltage ( $jAR$  in (17)) increases, chlorine production becomes less efficient because more oxygen is formed. Voltage increase occurs when  $R$  increases or more current is pushed through the reactor. This is consistent with experimental data on these competing reactions. Oxygen production has a lower free energy, however, chlorine production is kinetically favored (Karlsson & Cornell, 2016) As the driving force is increased, more oxygen is produced relative to chlorine. Equations (16) and (17) indicate that the fractional conversion of chlorine,  $\phi$  is inversely proportional to voltage.

Experimental data was collected under continuous  $\text{Cl}_2$  production at steady-state. The fractional yield of chlorine,  $\phi$  was calculated by dividing the chlorine production rate (as measured by chemical analysis) by the theoretical production rate of chlorine ( $\phi = 1$ ), where all current would result in chlorine production. Since the fractional conversion of chlorine is inversely related to voltage, experimental data was fit to an inverse function shown in Figure 18:

$$\phi = a + \frac{b}{V} \quad (18)$$

This data could be improved with more experimentation; however, it is a reasonable start.

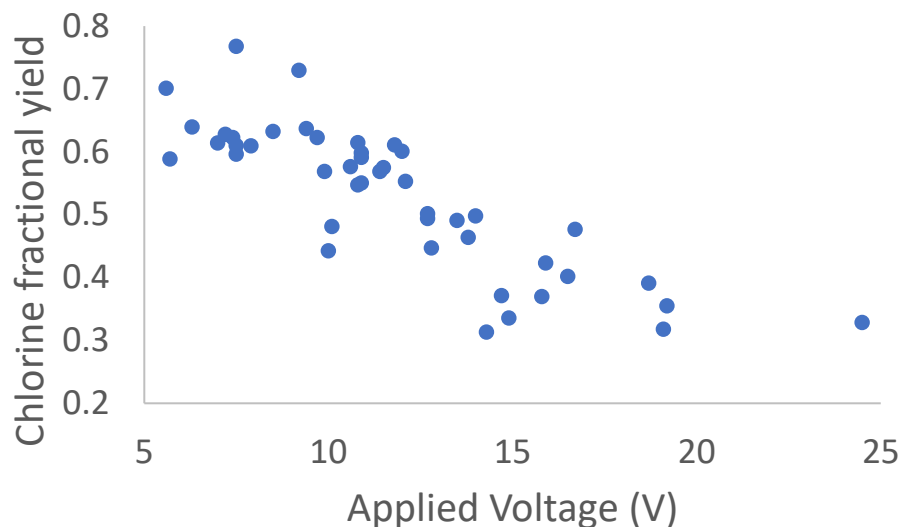


Figure 20. Voltage vs chlorine fractional yield

The rate model helps explain the relationship between energy use rates and current density for different salt concentrations as seen in Figure 16. As current is increased more voltage is required for the same electrolysis reactor. As seen in Fig. 20, as voltage increases the fractional yield of chlorine relative to oxygen is decreased. Data is shown for three different electrode surface areas:  $0.001425 \text{ m}^2$ ,  $0.000475 \text{ m}^2$ , and  $0.001350 \text{ m}^2$ . At lower salt concentrations this is more pronounced because of increased ohmic losses, requiring greater voltages for the same current flow compared to solutions with higher conductivity. In summary, as voltage is increased, fractional chlorine yield drops as more oxygen is produced which becomes more pronounced at lower salt concentration solutions.

The model indicates to maximize chlorine production relative to oxygen and use less energy, the voltage should be kept as low as possible. Using lower voltage would trade-off with electrode area, and detailed cost analysis is required to optimize. Additionally, reducing the ohmic resistance in the circuit would also allow more current to flow at lower voltages. Resistance can be lowered through reactor design and construction. Resistance can also be

lowered by increasing the salt concentration. Since salt is a consumable, this creates another economic tradeoff with electricity costs.

Laboratory experiments using two reactors in series and lowering the current by half in each one was compared to production using one reactor. Figure 21 shows data collected with flow rates of 70 mL/min at different salt concentrations. Using two reactors in series, each operating at lower voltages than a single reactor improves the electrical usage. For higher salt concentrations, the reduction in electrical use is ~35%. This shows the advantage of operating at lower voltages favoring chlorine production yields.

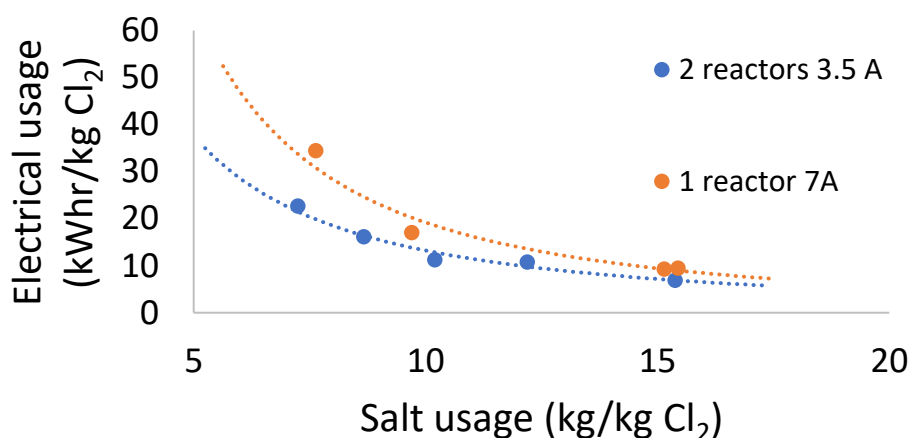


Figure 21. Reduction in energy use using increased reactor area at lower voltage.

### 3.8 Initial Trial Results

An on-site chlorination generator (Dirigo Stream) was fabricated at Maine Manufacturing Partners (MMP) and integrated into the Biddeford Pool Wastewater Treatment Plant in December 2022. Photographs of the equipment are shown in Figure 22. On the left is the NaCl supply tank. In the middle is the Dirigo Stream Unit with 4 electrolysis reactors. On the right is

the buffer tank. After expected integration challenges, the generator has operated continuously for up to 7 days (March 2023).

Current data collection includes plant flow rate, disinfectant metering flow rate, estimated salt use, and residual free chlorine measured inside the chlorination tank. Currently data collection is limited to manual collection. For a morning period, plant flow and respective chlorine metering flow is shown in Figure 23. As residents wake up, the plant flow increases for a morning peak, then decreases as the day proceeds. The disinfection metering rate was able to keep up with the plant changes. Figure 24 shows the salt use and the chlorine residual collected over the same time period. The residual chlorine is kept at or below 1 ppm as required by the State of Maine.



Figure 22. MMP Dirigo Stream Unit and buffer tank at Biddeford Pool Plant.

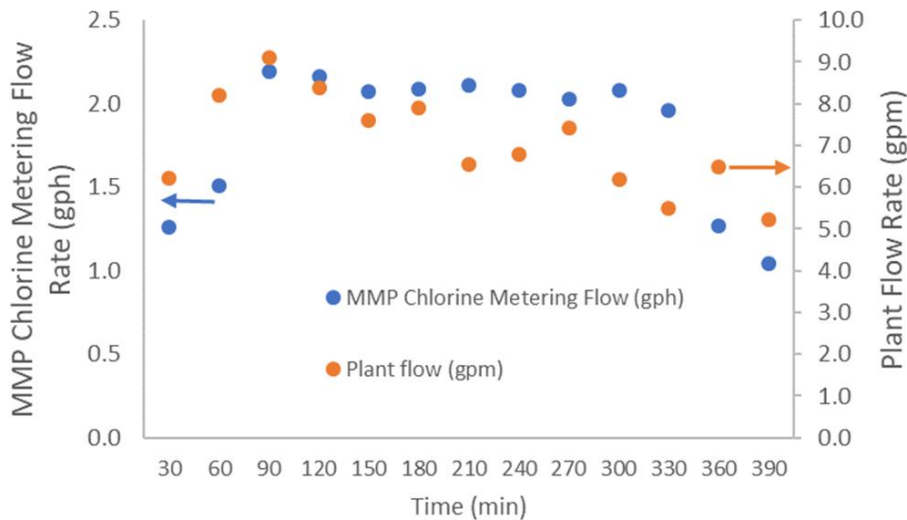


Figure 23. Plant flow and respective chlorine metering flow during morning hours at Biddeford Pool.

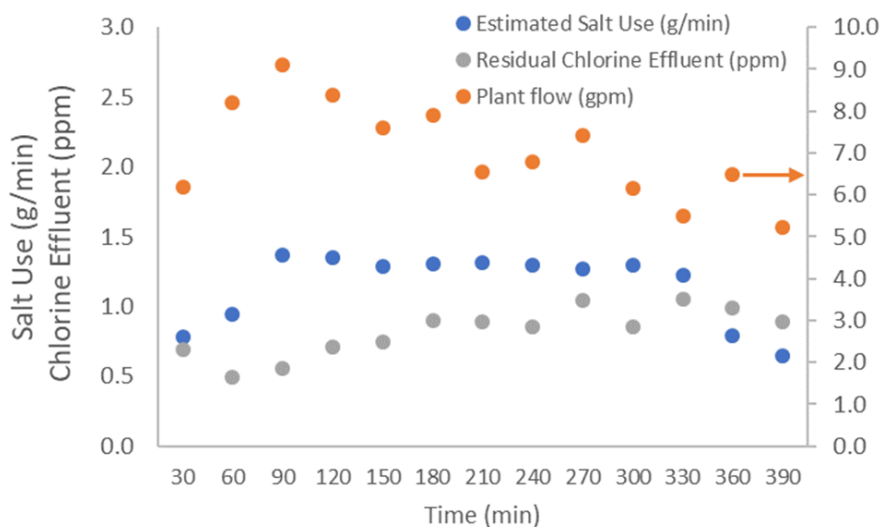


Figure 24. Corresponding salt use and residual chlorine for morning hours at Biddeford Pool.

### 3.9 Future Work

Ideally, the buffer tank would maintain constant chlorine concentration as chlorine is withdrawn and replaced with NaCl. One possibility is to use a chlorine sensor. Typical use of



these sensors is at low concentrations, 1-10 ppm, to make sure there is some extra chlorine available in disinfection applications. Higher concentration chlorine sensors (up to 2000 ppm) in the range of our expected buffer tank concentrations are harder to find.

A Walchem High Range Free  $\text{Cl}_2/\text{Br}_2$  was tested for installation and use. The sensor is quite sensitive to pH. An example is shown in Figure 25 for a 1800 ppm standard free chlorine sample measured at different pH with the sensor. This creates a burden for accurate pH measurement, within 0.1, in order to obtain a reasonable chlorine concentration reading. At this time, this method is not feasible or reliable to implement in a feedback control system to modulate the electrolysis reactors to produce more or less chlorine as demand changes.

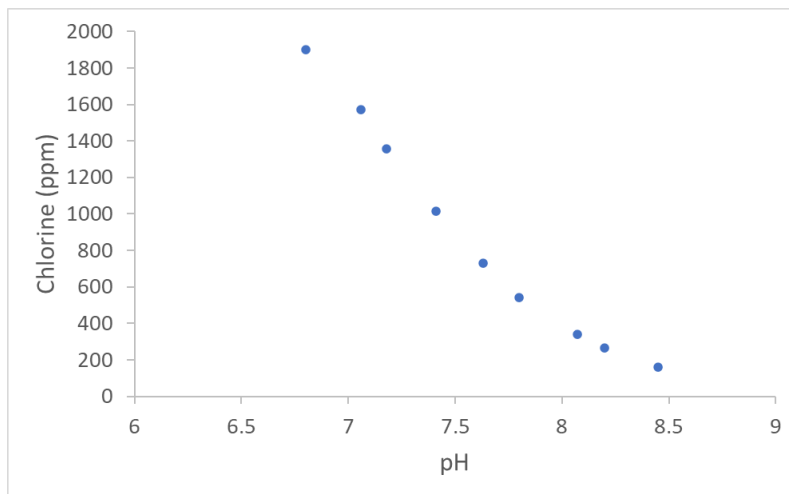


Figure 25. Sensitivity of chlorine reading to pH for Walchem high  $\text{Cl}_2$  sensor.

An alternative solution appears in the kinetic model above. If reactors can be produced and calibrated to specific standards, the fractional chlorine yield can be calculated during operation. Once this is determined, the production rate of chlorine can be calculated. This rate can be targeted to match the withdrawal rate required to disinfect. Future work will focus on

developing a system optimization process for minimizing inputs and ensuring smooth plant operation.

## CHAPTER 4

### HOCI FOGGING DISPERSION MODEL

#### 4.1 Introduction

The recent pandemic raised awareness of disinfection practices and applications. Dental offices understood the advantages of using hypochlorous acid as a disinfectant. Dental practices either purchased hypochlorous acid or purchased small-scale equipment to produce it on site. Hypochlorous acid is expensive to purchase, and equipment used to make small batches of hypochlorous acid has limitations. There remain many questions regarding local production of hypochlorous acid and utilizing it most effectively.

After interviewing dentists and observing practices, one application became clear. During dental procedures, fine fluid particles are generated that become dispersed in the operating room. These airborne particles are contaminated with viruses including COVID. The particulates are aerosols which can remain airborne for many hours. It was found that aerosols from speaking can remain stagnant in air for up to 9h (Ding, Teo, Wan, & Ng, 2021). If these particulates are not removed, concentrations could increase over time and spread infection.

One solution to this application is fogging hypochlorous acid to neutralize suspended virus particulates. Dental practices use hand-held foggers to disinfect the air after dental procedures. At concentrations near 200 ppm, hypochlorous acid is considered safe and non-toxic. It was found effective in decontaminating inert surfaces carrying noroviruses and other enteric viruses in a 1-minute contact time (Nguyen et al., 2021) and it could inactivate within 10 min avian influenza virus (AIV) immediately after spraying it for 10 sec (Hakim et al., 2015). It

would be optimal to design an automated system that could disinfect the room between procedures, freeing up assistants for other tasks.

As a starting point for system design, a model was initiated to explore the dispersion of fog in a room as a function of carrier gas velocity and position. The long-term goal is to couple the dispersion with evaporation and reaction of the hypochlorous acid fog with virus particles. The model should estimate the fogging time and concentration to disinfect a room. Initial results on hypochlorous fog dispersion are presented.

Droplets and aerosol are differentiated according to their behavior in the environment. Droplets are above 20 microns in size. They are usually produced during coughs, sneezes, shouting, etc. They succumb to gravity, meaning that they fall after travelling in the air for 1 to 2m. Aerosol on the other hand is made of particles under 10 microns in diameter and they can travel from many meters before they fall to the ground or some other surface (Medmastery, 2020).

## **4.2 Finite Element model**

COMSOL Multiphysics is a powerful interactive simulation environment used to model and solve all kinds of scientific and engineering problems. With COMSOL Multiphysics you can easily extend conventional models for one type of physics into Multiphysics models that solve couples' physics phenomena and that do simultaneously (COMSOL Multiphysics, 2014). This software was used to model the dispersion of hypochlorous acid droplets in a room. The following steps were set up: defining the dimension of the room, building geometry of the room, adding the physics (Laminar Flow and Transport of Diluted species), assigning constant

parameters, selecting the Mesh, computing the analysis and then creating plots under results section.

The geometry of the room was 5m in width and 3m in height Figure 26 with the inlet fogger dimension and location on the center of the left wall.

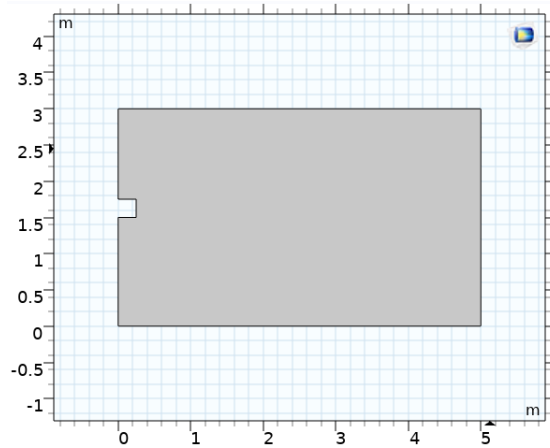


Figure 26. Geometry of a room and fogger location

The fog (HOCl aerosol) properties are summarized in table 2. The fog inlet and outlet are defined in Figure 25. The remaining boundary was the room wall.

Table 2. Fog properties

Fog density	1.307 kg/m <sup>3</sup>
Dynamic Viscosity	1.8 x 10 <sup>-5</sup> Pa.s
Inlet Velocity	0.5 m/s and 0.05 m/s

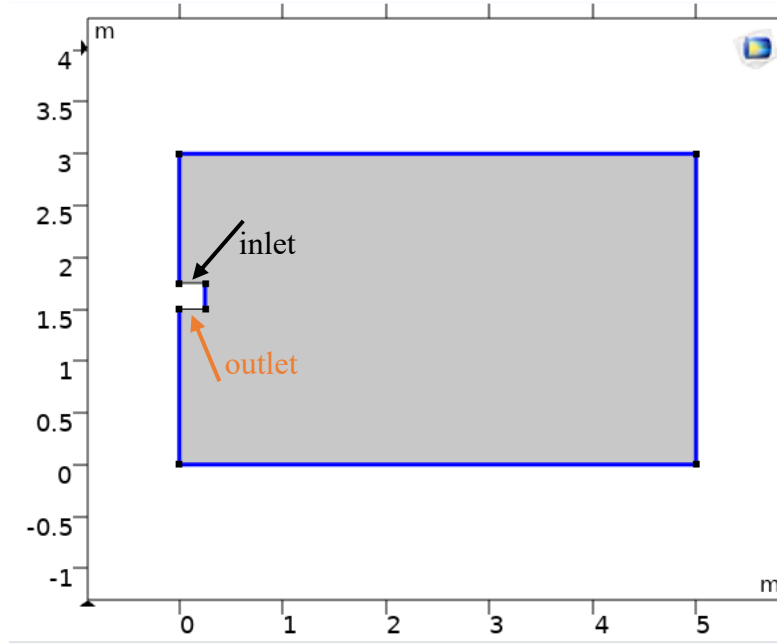


Figure 27. Boundaries of the room

The transport of diluted species interface provided an environment for reaction and transport of species by diffusion. The dependent variable is the molar concentration. The diffusion coefficient used was  $2.43 \times 10^{-12} \frac{m^2}{s}$ , it was calculated using the Stokes-Einstein equation 19.

$$D = \frac{k_b \times T \times C_c}{6 \times \pi \times r \times \eta} \quad (19)$$

where:

D: diffusion coefficient

$k_b$ : Boltzmann's constant

$C_c$ : Cunningham correction factor

r : solute radius

$\eta$  : solvent viscosity

T : temperature (K)

#### 4.2.2 Mesh size

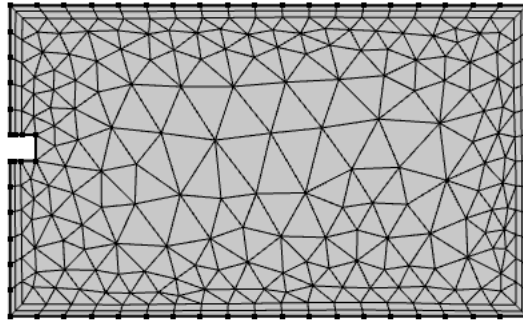


Figure 28. Extra Coarse mesh

### 4.3 Model Results

Figures 29 and 30 shows results for the fog dispersion in the room at different inlet velocities taken at 200 seconds after spraying. These results are for one inlet. The fog concentrates near the inlet and room coverage is sensitive to inlet velocity. Figure 31 indicates that at lower velocities of 0.05 m/s room coverage is quite poor even after 17 minutes of fogging.

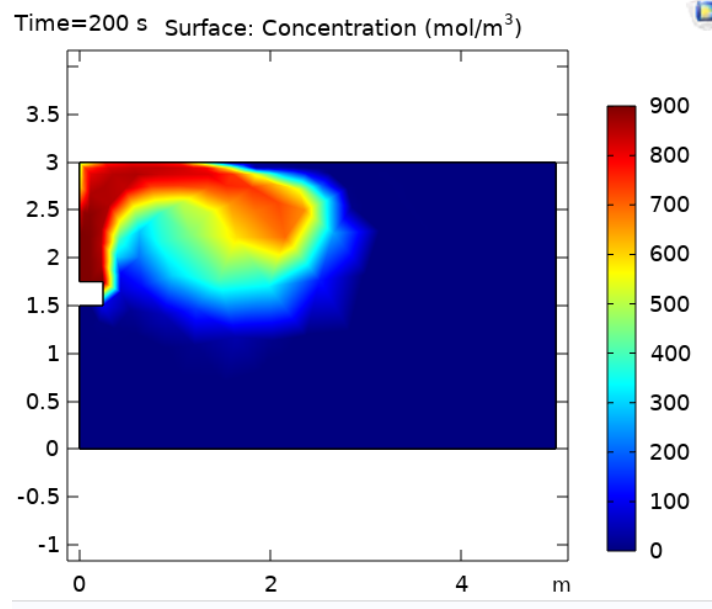


Figure 29. 1 fog inlet at 0.05 m/s inlet velocity

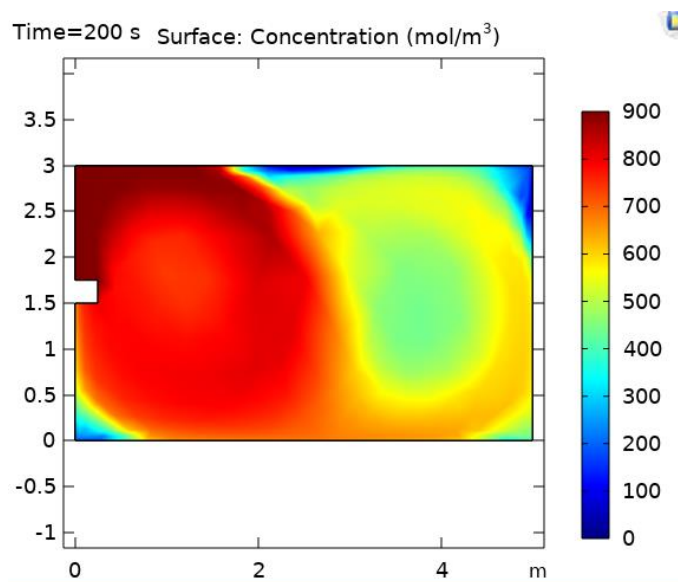


Figure 30. 1 fog inlet at 0.5 m/s inlet velocity



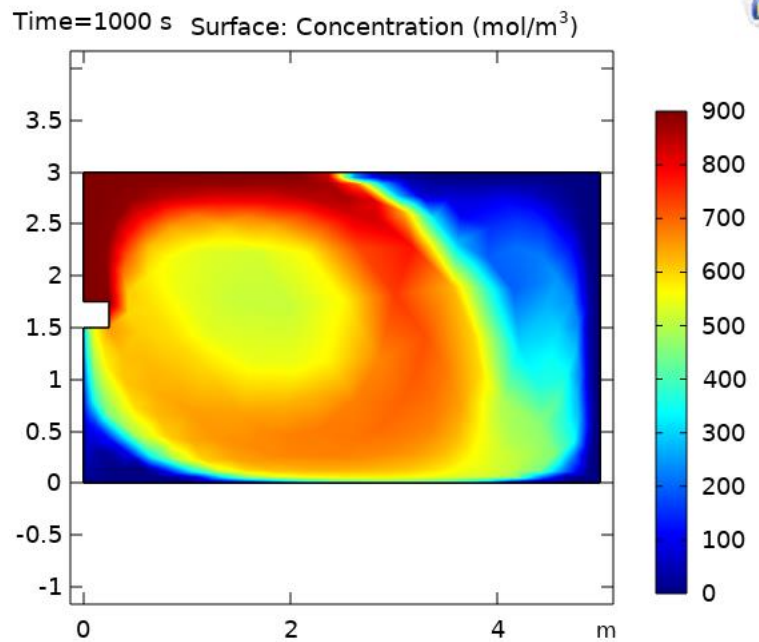


Figure 31. 1 fog inlet at 0.05 m/s velocity after 1000s~17min.

Figures 32 and 33 show the improvement in room coverage with a second fogging inlet.

Consistent with the single inlet, higher velocities provide better room coverage. In the case of fogging velocity of 0.5 m/s, the second inlet allows complete room coverage after 200 seconds, where no blue color is seen in the corners which would indicate zero coverage.

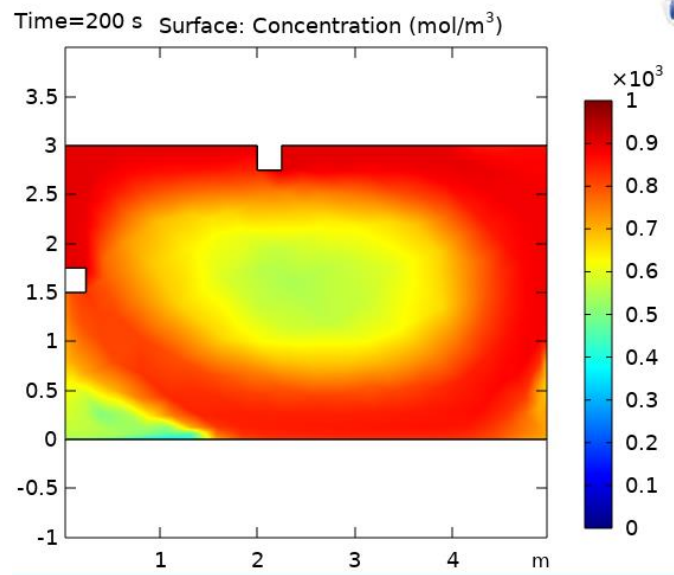


Figure 32. 2 fog inlets at 0.5 m/s inlet velocity

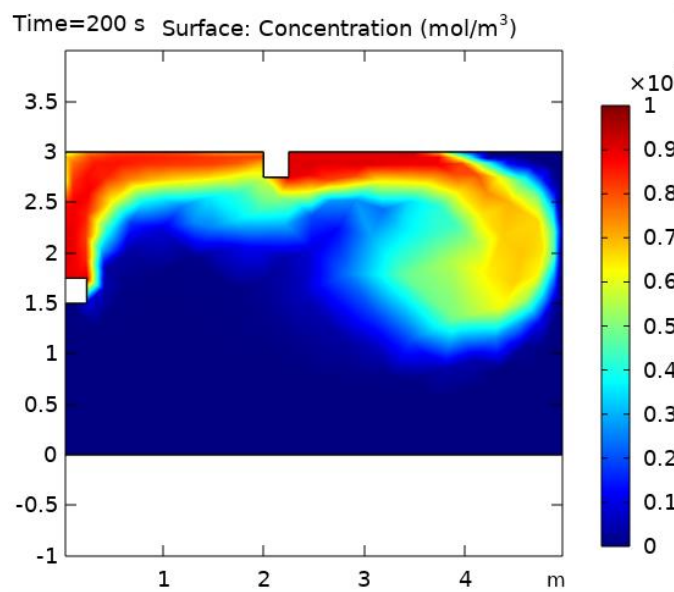


Figure 33. 2 fog inlets at 0.05 m/s inlet velocity

#### **4.4 Applications to Dental Clinic Applications**

The results above are preliminary work towards designing an effective fogging procedure to neutralize airborne pathogens in a Dental Clinic procedural room. The first step in designing an automated fogger is to demonstrate complete room coverage because dead spaces exist in room corners where airborne pathogens can accumulate. The disinfectant fog coverage is sensitive to injection velocity and location.

The next steps in design would include modeling the interaction between the fog and airborne pathogens as well as the evaporation of the droplets in the atmosphere. This would need to include some type of kinetic description of the reaction between the hypochlorous acid and the pathogens. In typical disinfection applications, the concentration of disinfectant multiplied by the application time is an important design parameter. Determining this would allow for the appropriate concentration of disinfectant and the exposure time to clean the room.

## CHAPTER 5

### CONCLUSIONS AND FUTURE RESEARCH DIRECTIONS

The COVID pandemic revealed weaknesses in the disinfectant supply chain stimulating local production solutions. Hypochlorous acid (HOCl) is a powerful disinfectant that is easily produced from the electrolysis of sodium chloride. A review of HOCl indicates a wide variety of applications. These include wound care, eye care, pet care, horticulture, and wastewater treatment.

One HOCl application focus of this work was wastewater treatment. A system was designed and tested for on-site disinfectant generation in a wastewater treatment plant to replace concentrated bleach produced centrally and delivered to the plant. The system was designed to use wastewater effluent and sodium chloride. The reactor performance was quantified using batch and continuous experiments. Energy and salt usage rates were determined relative to chlorine production. The experimental current yield of chlorine was determined for different current densities and sodium chloride concentrations.

Assuming the current can produce either chlorine or oxygen at the anode, a reactor model was developed that indicated an inverse correlation between current yield for chlorine and applied voltage. This correlation can be used to estimate chlorine production based on system inputs. This is useful for operating a system that maintains constant concentration of chlorine used for disinfection and assuring smooth plant operation.

The model also guides design and operation based on economics. If accurate capital costs for each reactor are available, reactors can be configured to accomplish disinfection demand at reduced voltages and operating at higher chlorine yields, optimizing capital and operating cost

minimization. This can be used for real-time system optimization as chlorine demand in the plant varies throughout the day, storm events, and season.

A second HOCl application explored was removal of airborne pathogens in a dental clinic by fogging. Observations were made of dental surgeries and subsequent disinfection of procedure rooms which included fogging. In efforts to design a fogging system, a finite element model was developed to predict room coverage with HOCl fog as a function of fog carrier velocity and inlet location. Results allow determining the time required to completely cover the room with fog as a function of carrier velocity and number of inputs. The next step would incorporate a kinetic model for HOCl fog destruction including reaction and evaporation.

## REFERENCES

- Ampiauw, R. E., Yaqub, M., & Lee, W. (2021). Electrolyzed water as a disinfectant: A systematic review of factors affecting the production and efficiency of hypochlorous acid. *Journal of Water Process Engineering*, 102228.
- Bahoshy, D. L. (2018). Hypochlorous acid for Dry Eye and Blepharitis. Stoney Creek, ON, USA.
- Bajgai, J., Kim, C.-S., Rahman, M., Fadriquel, A., Thuy, T. T., Song, S.-B., & Lee, K.-J. (2020). Application of New Concept Disinfectant, Huureka®, On Livestock Farming Application of New Concept Disinfectant, Huureka®, On Livestock Farming. *Korean Journal of Waters*, 1-12.
- CleanLink. (n.d.). Understanding Hypochlorous Acid (HOCl). *CleanLink*.
- Clieron. (2021, July). Retrieved from Clieron wound and skin care: <https://www.clieron.com/blogs/animal-care-tips/top-10-benefits-of-hypochlorous-acid-wound-care>
- COMSOL Multiphysics Reference Manual Version 5.5. (2019).
- Digital Titrator Manual, Model 16900. (2013).
- Ding, S., Teo, Z. W., Wan, M. P., & Ng, B. F. (2021). Aerosol from speaking can linger in the air for up to nine hours. *PubMed Central*.
- HOCl Inside. (2023, April 4). Retrieved from <https://hoclinside.com/>
- Karlsson, R. K., & Cornell, A. (2016). Selectivity between Oxygen and Chlorine Evolution in the Chlor-Alkali and Chlorate Processes. *Chemical Reviews*, 116(5).
- Medmastery (Director). (2020). *COVID 10: Is COVID-19 an airborne disease? Will we all need to wear face-masks against SARS-CoV-2?* [Motion Picture].
- Pescod, M. (1992). Food and Agriculture Organization of the United Nations. Rome.
- Phillips, R., Edwards, A., Rome, B., Jones, D. R., & Dunnill, C. W. (2017, September 13). Minimising the ohmic resistance of an alkaline electrolysis cell through effective cell design. *International Journal of Hydrogen*, 42(38), 23986-23994.
- School, W. S. (2018). Biochemical Oxygen Demand (BOD) and Water. *USGS*.
- Urushidani, M., Kawayoyoshi, A., Kotaki, T., Saeki, K., Mori, Y., & Kameoka, M. (2022, April 7). Inactivation of SARS-CoV-2 and Influenza A virus by dry fogging hypochlorous acid solution and hydrogen peroxide. (E. Ito, Ed.) *PLOS ONE*, 17(4), 1-14. doi:<https://journals.plos.org/plosone/article?id=10.1371/journal.pone.0261802>
- Wang, L., Bassiri, M., Najafi, R., Yang, J., Khosrovi, B., Hwong, W., . . . Robson, M. (2017). Hypochlorous acid as a Potential Wound Care Agent. *Journal of Burns and Wounds*.

- Hakim, H., Thammakarn, C., Suguro, A., Ishida, Y., Kawamura, A., Tamura, M., Satoh, K., Tsujimura, M., Hasegawa, T., & Takehara, K. (2015). Evaluation of sprayed hypochlorous acid solutions for their virucidal activity against avian influenza virus through in vitro experiments. *Journal of Veterinary Medical Science*, 77(2). <https://doi.org/10.1292/jvms.14-0413>
- Ishihara, M., Murakami, K., Fukuda, K., Nakamura, S., Kuwabara, M., Hattori, H., Fujita, M., Kiyosawa, T., & Yokoe, H. (2017). Stability of weakly acidic hypochlorous acid solution with microbicidal activity. *Biocontrol Science*, 22(4). <https://doi.org/10.4265/bio.22.223>
- Nguyen, K., Bui, D., Hashemi, M., Hocking, D. M., Mendis, P., Strugnell, R. A., & Dharmage, S. C. (2021). The potential use of hypochlorous acid and a smart prefabricated sanitising chamber to reduce occupation-related COVID-19 exposure. In *Risk Management and Healthcare Policy* (Vol. 14). <https://doi.org/10.2147/RMHP.S284897>
- Perry, S. C., Ponce de León, C., & Walsh, F. C. (2020). Review—The Design, Performance and Continuing Development of Electrochemical Reactors for Clean Electrosynthesis. *Journal of The Electrochemical Society*, 167(15). <https://doi.org/10.1149/1945-7111/abc58e>

### **BIOGRAPHY OF THE AUTHOR**

Deborah Ngabanyi Sebagisha was born in the Democratic Republic of Congo (DRC). She graduated from Lycée Amani High School in Goma (DRC) in July 2016. In May 2021, she graduated from the University of Maine with a Bachelor of Science degree in Chemical Engineering. Deborah is a candidate for the Master of Science degree in Chemical Engineering from University of Maine in May 2023.



ProQuest Number: 30667074

INFORMATION TO ALL USERS

The quality and completeness of this reproduction is dependent on the quality and completeness of the copy made available to ProQuest.



Distributed by ProQuest LLC (2023).

Copyright of the Dissertation is held by the Author unless otherwise noted.

This work may be used in accordance with the terms of the Creative Commons license or other rights statement, as indicated in the copyright statement or in the metadata associated with this work. Unless otherwise specified in the copyright statement or the metadata, all rights are reserved by the copyright holder.

This work is protected against unauthorized copying under Title 17,  
United States Code and other applicable copyright laws.

Microform Edition where available © ProQuest LLC. No reproduction or digitization of the Microform Edition is authorized without permission of ProQuest LLC.

ProQuest LLC  
789 East Eisenhower Parkway  
P.O. Box 1346  
Ann Arbor, MI 48106 - 1346 USA